Chapter 3
Water Absorption of Plant Aggregate

Sofiane Amziane, Vincent Nozahic and Mohammed Sonebi

Abstract In "agro-concretes", highly-porous plant-based particles are used, and are responsible for massive water absorption.

Keywords Plant aggregate · Water absorption · Wettability · Porous medium · Filtration · Absorption model

3.1 Introduction

In "agro-concretes", highly-porous plant-based particles are used, and are responsible for massive water absorption. It is often reported (Nguyen et al. 2010; Arnaud and Gourlay 2012) that this hydrophilic nature of the plant materials leads to competition with hydraulic binders, which require at least a certain amount of water in order to form hydrate products and cohesion. Such competition appears to be the reason for the crumbling of hydraulic binders (Cerezo 2005). Binders with high carbonation potential—in particular, aerated-lime-based binders—are often employed to counter this problem, at least on the surface of the agro-concrete (Elfordy et al. 2008; Mounanga et al. 2009; Nguyen et al. 2009a).

Recent studies performed on self-compacting concretes (Kwasny et al. 2012) could help better under the amount of water that needs to be added to the particulates in order to limit competition between the absorption of the plant material and the hydration of the binder (Jacek et al. 2012; Diederich et al. 2010). Indeed, the pre-wetting methods used up until now to provide the water necessary to saturate the granulates and the binder cannot really justify the dosage of water to be used

S. Amziane (✉) · V. Nozahic
Institut Pascal, Clermont Université, Clermont-Ferrand, France
e-mail: sofiane.amziane@univ-bpclermont.fr

M. Sonebi
School of Planning, Architecture and Civil Engineering,
Queen's University Belfast, Belfast, UK

S. Amziane and F. Collet (eds.), *Bio-aggregates Based Building Materials*,
RILEM State-of-the-Art Reports 23, DOI 10.1007/978-94-024-1031-0_3

(Cerezo 2005; Nguyen et al. 2009a). In addition, the fabrication of the agroconcrete also comes into play, as the method of compaction is used, partially crushing the plant material and thereby releasing some of the mix water (Nguyen et al. 2009b).

3.2 Wetting of Porous, Heterogeneous Surfaces

Whether in the binder, in the lignocellulosic particles or at the interface between those two entities, water transfer by means of capillary phenomena and diffusion in the plant structure play a very important role. However, that transfer can only take place after the *wetting of the plant surface* by the interstitial water contained in the binder.

A surface's *wettability*, where the main characteristic is its surface tension γ_S, is a crucially-important concept when the adhesion of a liquid (which has a surface tension γ_L) to that surface is needed to be calculated. In the particular case of a cement paste applied to a plant particle, the process of adhesion mainly occurs between the interstitial liquid and the surface of the plant.

Wettability, which is necessary for any process of adhesion, can be examined on two different scales:

- *The physical intermolecular bonds*: There are two types of bonds created by the wetting of a plant surface with an aqueous solution: hydrogen bonds (which are OH bonds) and van der Waals bonds (electrostatic forces exerted between the particles).
- *The physical measurements (contact angle and surface tension)*: these measured values physically describe the expression of the bonds within each of the media (surface tension for the liquid and the solid) and at equilibrium between two (surface tensions of the solid and liquid γ_{SL}) or three media (Young–Dupré law defining the contact angle).

3.2.1 Surface Tension and Interface Tension

A molecule of water or of any other liquid, when it is situated within that liquid, is subject to van der Waals-type forces of cohesion, exerted isotropically upon it. On the other hand, when the molecule is at the boundary between the air and the liquid, it is in a slightly higher state of energy, which creates a stress of tension (expressed in N m^{-1} or J m^{-2}). This interfacial tension between a liquid and a gas is called the *surface tension* γ_{LG}. The surface tension of water in air at 20 °C, for example, is 72.7×10^{-3} N m^{-1}. The surface of a solid in contact with a gas is an instability of the same type. It is known as the surface energy of *surface tension* γ_{SG} of the solid.

When a solid and a liquid brought into contact with one another, where each of them has a surface energy with the air or any other surrounding gas, a new

interfacial equilibrium is created. That equilibrium is an energy balance between the liquid–gas surface tension γ_{LG}, the solid–gas surface tension γ_{SG} and the *interfacial tension* γ_{SL}. An adhesion energy known as the Dupré energy, E_{DUPRE} (expressed in N m^{-1} or J m^{-2}), is then defined:

$$E_{DUPRE} = \gamma_{LG} + \gamma_{SG} - \gamma_{SL} \tag{3.1}$$

3.2.1.1 Contact Angle and Wettability

General laws

When a drop of liquid is placed on a smooth, solid surface, it undergoes spreading to a greater or lesser degree, which is the resultant of the surface energies. This wettability of the surface can be defined by the so-called *spreading coefficient* S (de Gennes et al. 2004):

$$S = \gamma_{SG} - \gamma_{SL} - \gamma_{LG} \tag{3.2}$$

When the value of the coefficient S is greater than 0, the total wetting of the surface can be observed. On the other hand, if S is negative, a *partial wetting can be seen*, leading to the formation of a drop sitting on the solid surface. As a general rule, the lower the liquid's surface tension, the greater the spreading. As water has a high surface tension, the wetting of a solid by water is generally incomplete.

In the case of partial wetting, the *Young–Dupré law* gives the expression of the static *contact angle* θ of a liquid drop placed on a solid substrate, at equilibrium with the vapour phase:

$$\cos\theta = \frac{\gamma_{SG} - \gamma_{SL}}{\gamma_{LG}} \tag{3.3}$$

This relation is obtained by projection of the vectors formed by the interfacial tensions taking the triple point (Fig. 3.1b) as the origin. The following situations may be encountered:

- $\theta > 90°$: The liquid is said to be "non-wetting". In the case of water, the solid is said to be hydrophobic (Fig. 3.1b);
- $\theta < 90°$: The liquid is said to be "wetting". For water, the solid is said to be hydrophilic (Fig. 3.1a).

Wetting of a heterogeneous and porous lignocellulosic plant surface

The surfaces representative of lignocellulosic particles exhibit numerous heterogeneities and significant roughness (Gardner et al. 1991). The wetting of wood and the factors influencing it have been widely studied over last decades (Gardner et al. 1991; Walinder 2000; Bruyne 2008). Generally speaking, the rougher its surface, the larger will be the contact angle formed by a hydrophobic

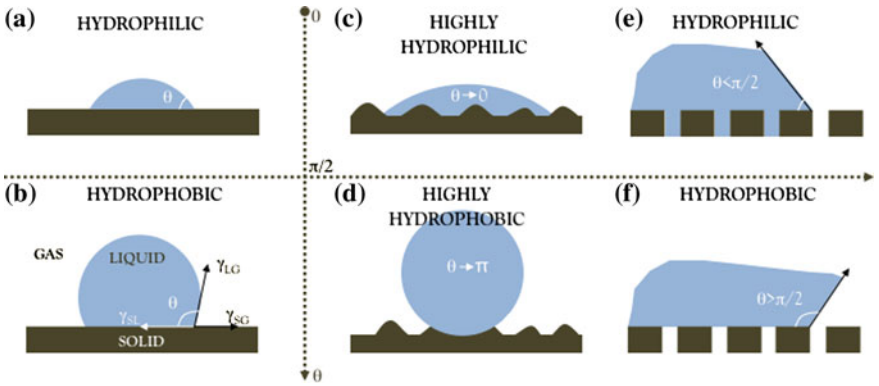

Fig. 3.1 Diagrammatic representation of: a hydrophilic (**a**) and hydrophobic (**b**) smooth surface; a hydrophilic (**c**) and hydrophobic (**d**) rough surface; and a hydrophilic (**e**) and hydrophobic (**f**) porous surface (de Gennes et al. 2004)

material (de Gennes et al. 2004) (Fig. 3.1d). Similarly, the rougher the surface of a *hydrophilic material such as wood*, the more likely it is to be perfectly wettable (Fig. 3.1c).

3.3 Transfer Phenomena in a Porous Medium

3.3.1 Liquid Transfer in the Laminar Regime

3.3.1.1 Capillary Transfer

When the aqueous mineral binder comes into contact with a hydrophilic porous support such as a lignocellulosic particle, its constituting water will wet the surface to which it is applied. Thus, as a function of the size of the pores in the support, a capillary pressure of suction P_C is exerted on the free water in the binder. That pressure P_C [N m^{-2}] is characterised by the *Kelvin–Laplace law*:

$$\mathbf{P_C} = \frac{-2\gamma_{\mathbf{LG}}.\cos\theta}{\mathbf{r}} \tag{3.4}$$

γ_{LG}: surface tension of the liquid (here the free water in the binder) on contact with the surrounding gas [N m^{-1}]
θ: contact angle which the liquid forms with the porous surface
ρ: radius of the capillary pore in question [m]

Thus, the height by which the liquid rises in the capillary h_L defined by *Jurin's law* can be calculated:

$$\mathbf{h_L} = \frac{-\mathbf{P_C}}{\boldsymbol{\rho}_\mathbf{L}.\mathbf{g}} \tag{3.5}$$

g: acceleration due to gravity [m s^{-2}]
ρ_L: density of the liquid (here the free water in the binder) [kg m^{-3}]

The dynamics of that ascension is defined by *Washburn's law*, which establishes a relation of *proportionality* between the capillary rise height h_L *and the square root of the elapsed time.* In particular, it is influenced by the fluid's dynamic viscosity μ:

$$\mathbf{h_L^2} = \frac{\mathbf{r}.\gamma_{\mathbf{LG}}.\mathbf{cos}\theta}{\mathbf{2}\mu}.\mathbf{t} \tag{3.6}$$

μ: Dynamic viscosity [Pa s]

3.3.1.2 Filtration Transfer in a Saturated Porous Medium

In the complex porous medium represented by agroconcretes, the pressure generated by capillary water absorption triggers a second phenomenon at the interface between the binder and the particles. Indeed, this absorption engenders a *phenomenon known as filtration* of water through the large mineral granulates (>50 μm) which make up the binder. This aqueous movement in a saturated medium, which is predominant at the interface, may bring fine particles and ions suspended in the interstitial liquid into the plant structure. The filtration process is similar to the laminar flow of a viscous interstitial fluid, undergoing friction as it passes over the granular skeleton of the binder. It is defined by *Darcy's law*:

$$\vec{\mathbf{u}} = \frac{-\mathbf{k}}{\mu}(\overrightarrow{\boldsymbol{P_C}} - \rho\vec{\mathbf{g}}) \tag{3.7}$$

$\vec{u}$: Rate of filtration [m/s]
P_C: Pressure [Pa]
ρ: Density of the fluid [kg m^{-3}]
$\vec{g}$: Vector of acceleration due to gravity [m s^{-2}]
k: Intrinsic permeability [m^2]

3.3.2 Transfer of Water Vapour, Particles or Ions by Diffusion

There are many different types of diffusion phenomena, which occur in numerous media. Agroconcretes, though, are a good example, because from the moment they are made, they are subject to numerous diffusive transfers, such as:

- the *diffusion of liquid water* into the plant cell walls from the moment of mixing to an age of several days;
- the diffusion of mineral particles from the binder and plant extractible materials into the mix water—particularly at the binder/plant interface;
- the *diffusion of water in vapour form as the concrete dries*, over the course of 1–3 months, but also during the use of the material.

All these phenomena have an influence on the short- and long-term adhesion between a lignocellulosic particle and a mineral binder. Thus, the diffusion of liquid water into plant cell walls may, potentially, destroy the hydrogen bonds established with the binder (Coutts and Kightly 1984; Vick 1999) and cause the plant tissues either to swell or to retract (Rowell 2005).

3.3.2.1 Fick's Law

The numerous diffusive phenomena observed in nature are described by *Fick's laws*, and can be characterised by their *diffusion coefficient D*. These are very common transport phenomena, usually engendered by the creation of a gradient of chemical potential, hydric gradient or concentration gradient. Diffusion tends to even out that gradient, in accordance with Fick's first law:

$$\mathbf{J} = \mathbf{D}.\frac{\partial \boldsymbol{C}}{\partial \boldsymbol{x}} \tag{3.8}$$

J: Diffusive flow [mol m^{-2} s^{-1}]
D: Diffusion coefficient [m^{-2} s^{-1}]
C: Concentration of molecular species [mol m^{-3}]
X: Spatial coordinate where diffusion is observed [m]

Consider the end of a wood core sample, stabilise in an atmosphere of relative humidity RH_0, brought into contact with an atmosphere of HR_1 at a time t = 0. A gradient of humidity concentration C(x,t) is instantaneously created with the wood tissues, giving rise to a diffusion front whose depth is d(t). The Brownian nature of the motion accounts for the *progress of the diffusion front d proportional to the square root of elapsed time*.

3.3.2.2 Einsteinian Laws

The diffusion of the extractible materials and mineral particles in the interstitial liquid medium is responsible for problems with the setting of the mineral binder in contact with a plant particle. This migration of species is governed by the Einstein–Smoluchowski law (Einstein 1905), which defines the Brownian motion of the particles.

$$\mathbf{D} = \boldsymbol{\mu_0}.\mathbf{K_B}.\mathbf{T} \tag{3.9}$$

D: diffusion coefficient
K_B: Boltzmann's constant
T: Temperature of the medium [K]
μ_0: Mobility of the particle, of the ion, etc.

An important special case of this law defines the diffusion of spherical particles in a medium with a low Reynolds number (laminar regime): this is the Stokes–Einstein law (Bentz et al. 2009):

$$\mathbf{D} = \frac{\mathbf{K_B}.\mathbf{T}}{\mathbf{6}\pi.\mu.\rho} \tag{3.10}$$

μ: Dynamic viscosity of the medium [Pa s]
ρ: Radius of the particle diffusing in the medium [m]

This relation is applicable in the capillaries of lignocellulosic stalks and the pores of cell walls, due to their very small diameter, meaning that their Reynolds number with water is less than 2400.

3.4 Analogy with Adhesion of Mortars to a Porous Support

A comparison can be drawn between the lignocellulosic wood granulates of "hempcrete" and a porous substrate (adherent) to which a mortar or flagging (adhesive) is applied. In order to illustrate this, firstly, there is need to set out the initial *hypotheses* that the *granulate is inert and dimensionally stable*. It is on these hypotheses that our discussion in this section is founded.

3.4.1 Capillary Absorbency of a Porous Support

With regard to the establishment of a short-term physical bond, liquid transfers by means of the *forces of capillarity* are of great importance. Numerous studies have

demonstrated the influence of the capillary absorption properties of the porous substrate on the development of bonding forces at the mortar/substrate interface (Groot and Larbi 1999; Courard 2000; Sugo et al. 2001).

Courard (2000) defines these capillary exchanges the *absorbency* of the substrate for the interstitial liquid in the mortar. If the absorbency is not high enough, the segregation of water on the surface of the substrate is observed which led to an increase in the final porosity of the interface.

Groot and Larbi (1999) describe the existence of an *optimal capillary absorption coefficient* with which maximal properties are achieved. They introduced the concept of the initial rate of absorption (IRA [kg m^2 min^{-1}]), which is defined as the capacity for capillary absorption per minute of the porous substrate placed in 3 mm of water. The optimum IRA is defined as being that which delivers the highest bond strength between the porous support and the mortar (2). Given that the IRA depends upon the volume and pore size, the authors stress that it is not the only influential factor. This observation is also reported by Sugo et al. (2001).

Sugo et al. (2001) described the *suction potential* existing between a relatively dry porous substrate and a water-saturated mortar, which tends to balance out. The moment the materials are brought into contact, the substrate's great suction potential causes the transport of the interstitial fluid from the mortar toward the substrate/mortar interface, and then into the actual pores of the substrate. In the view of those authors, over the course of these exchanges, gradients of humidity and of suction potential are established at the interface. As the binder becomes hydrated, the gradients evolve and may, depending on the size and interconnectivity of the porous structure, cause a backward flow of liquid from the support to the mortar, facilitated by large pores in the support (Groot and Larbi 1999; Sugo et al. 2001). This backflow may give rise to a regain in hydration (Fig. 3.2).

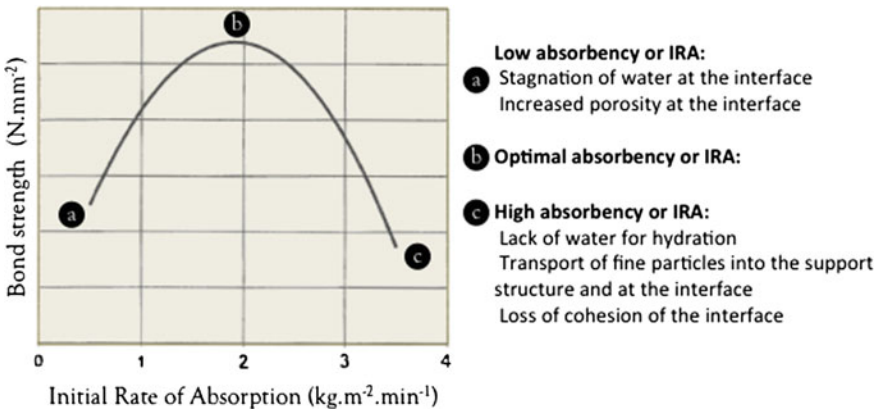

Fig. 3.2 Illustration of the optimum initial rate of absorption (Groot and Larbi 1999)

3.4.2 *Transport of Particles During Filtration*

Many authors reported the point that the processes of capillary absorption are responsible for the transport of fine particles in suspension from the mortar toward the surface and the porous structure of the substrate (Groot and Larbi 1999; Coutts and Kightly 1984; Sugo et al. 2001). Sugo et al. (2001) introduced the concept of a cluster of fine particles from the binder, which stagnate along the brick/mortar interface, providing continuity between the two materials. Excessive transfer would, in their view, lead to the fragilisation of the area of mortar situated before the interface, notably rendering it more porous. Conversely, an insufficient quantity would create an interface which was fragile because of poor interpenetration.

Groot and Larbi (1999) reported that these movements of fine particles from the mortar and their densification at the mortar/support interface are likely to substantially alter the capillary pressures exerted by the mortar.

3.5 Overview of the Processes of Binder/Wood Adhesion

The complexity of wood as a material—one which is highly hydrophilic, porous, subject to swelling, aniso-tropic and heterogeneous—accounts for the multitude of phenomena needing to be taken into account in order to understand its interaction with an adhesive (Coutts and Kightly 1984). The main interactions which take place in the specific case of the short-term adhesion of a mineral binder to wood are illustrated in Fig. 3.3. The important points which must be borne in mind are as follows:

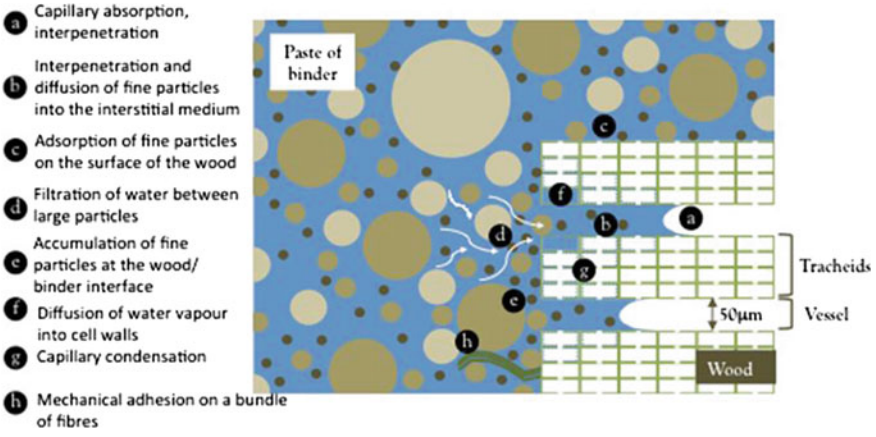

Fig. 3.3 Illustration of the interactions between a hydrated mineral binder and a particle of wood with which it is brought into contact after wetting

- Ensure optimal wetting which facilitates the interpenetration of the binder into the rough surface and the internal pores of the particles (vessels);
- Encourage as many physical bonds as possible, and interpenetration;
- Tend toward hydric transfers which are neither too great (lack of water for hydration) nor too slight (stagnation of water at the interface), by regulating the capillarity or filtration;
- Limit the filtration of fine particles from the binder toward the interface so as to prevent the buildup of particles;
- Limit the diffusion of particles from the binder into the interstitial liquid so as to limit concentration gradients;
- Limit the effects of the variations in the volume of the wood so as to ensure the interface is durable

3.5.1 Hygroscopic Behaviour When Immersed

The hygroscopic behaviour of lignocellulosic plant materials is due, in no small part, to their hydrophilicity. Their complex architecture is marked by multi-scale porosity, designed to carry the fluids necessary for them to flourish (sap and water). Even after cutting and transformation, this porosity continues to play its part, and thus is the primary channel of water absorption in accordance with Laplace's laws. This absorption takes place primarily in the conductive vessels or tracheids before the water propagates to the rest of the cells by diffusion across blockages and cell walls.

3.5.2 Water Absorption/Adsorption by Immersion

Immersion of dispersed granulates

Measuring the gravimetric rate and the rate of water (W) absorption and adsorption is crucially important in formulating plant-based concretes. The plant particles are first steamed at 60 °C for 48 h. For each experiment, m_0 = 50 g of dry plant material is used. The plant particles whose absorption we wish to measure are placed in a meshed recipient (a net, a grid, etc.) that allows the rapid evacuation of the soaking water and some of the interstitial water. The whole setup is then submerged for a period t = {1, 2, 5, 10, 30 min or 48 h} before being removed and manually wrung. The exact procedure is illustrated by Fig. 3.4. It is worth noting that this procedure does not allow the evacuation of part of the water which is present between the particles during wringing, or of the water adsorbed to the surface. Therefore, it is not possible to distinguish between absorbed water inside the capillaries and the water adsorbed to the surface. In addition, the manual

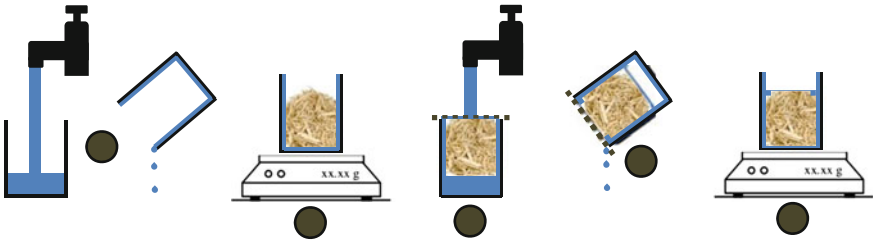

1. Fill the recipient with water and drain it;
2. After taring the balance, weigh out $m_0 = 20$ g of dry granulated material (60 °C, 48 h) into the damp recipient;
3. Cover the recipient with a sieve and fill with water through the sieve;
4. After a given period of immersion, drain the recipient through the sieve, taking care to shake it and achieve maximum evacuation of the water;
5. Wipe the walls of the recipient and weigh it on the balance whose tare has not been altered (*m(t)*).

Fig. 3.4 Step-by-step method for measuring the absorption/adsorption of plant particles by immersion

wringing engenders a not-insignificant degree of uncertainty, mainly when the experiment is of short duration.

$$W(t) = \frac{m(t) - m_0}{m_0}.100 \tag{3.11}$$

For each given duration, the measurement is repeated three times—in total, 18 tests—giving an absorption curve W(t) for a given particulate material. The maximum absorption rate WSAT is defined at 48 h.

Immersion of chips of known dimensions

The water absorption of chips of dimensions [2–3] × 7 × 60 mm^3, was analysed in parallel to that carried out on granulates. In each experiment, 5 chips are weighed and measured in the dry state before being submerged in water. Their mass is measured using a balance with precision of (±0.1 mg) after 5 min, and after 4, 14, 24, 38 and 48 h.

Tangential swelling of chips

The tangential swelling of immersed plant particles gives an idea of their capacity for deformation when brought into contact with water. Lignocellulosic plants, indeed, have the property of being able to integrate molecules of water or any other solvent into their very structure—notably due to the creation of hydrogen bonds (Rowell 2005). It is for this reason that we must allow freshly-cut wood to

dry (and therefore shrink) before using it. This measurement is perfectly complementary to the measurement of water absorption by immersion.

It should be noted that the natural character of plants and the limited dimensions of the transformed granulates (<1 cm for the width of a particle) means that it cannot accurately determine this parameter. For each type of granulate, therefore, the measurement is performed on 10 particles taken from the stem, with dimensions of [2–3] × 7 × 60 mm^3. It is therefore too demanding in terms of equipment to monitor the swelling using automated systems. The callipers with a resolution of ± 0.01 mm is selected. With untreated hemp and sunflower stalks, the measurements were taken at regular intervals up to 48 h.

The tangential swelling is expressed simply:

$$G_T(t) = \frac{1(t) - 1_0}{1_0}.100 \tag{3.12}$$

Maximum swelling GT MAX is considered to have been achieved after 48 h.

Wettability

The measurement of the contact angles seems to partly contradict the IRTF analyses presented in the previous section (Fig. 3.5a). Thus, the surface that proves most hydrophilic at the moment of deposition of the drop is the sunflower epidermis (76°), with the internal surface being initially quasi-hydrophobic (86°). This is attributable to a very rough surface on the internal face of the sunflower which, for a short period of time, keeps the drop spherical (Fig. 3.5c). For defibred hemp plant granulate, few differences are visible at the moment the drop is deposited: both faces are initially hydrophobic ($\theta > 90°$).

The major differences in terms of the wetting behaviour can be seen after 60 s. The surfaces of the epidermal faces lead to a gradual and limited spreading of the deposited drop (Fig. 3.5b). The behaviour of the internal surfaces is very different because, very quickly, the drop undergoes significant spreading and is then absorbed into the structure of the particle (Fig. 3.5c). This observation can be linked to the internal faces' high content of hemicellulose, which is extremely hydrophilic. In order for the plant to survive, the primary cell walls situated inside of the stem—particularly in the marrow—are composed of hydrophilic substances (cellulose, hemicellulose).

3.5.3 Behaviour in Terms of Water Adsorption/Absorption

Adsorption/absorption and swelling of chips

Before truly turning our attention to the behaviour of the transformed granulates when immersed, preliminary information can be gleaned by examining a single chip. With this goal in mind, chips of hemp and sunflower ([2–3] × 7 × 60 mm^3)

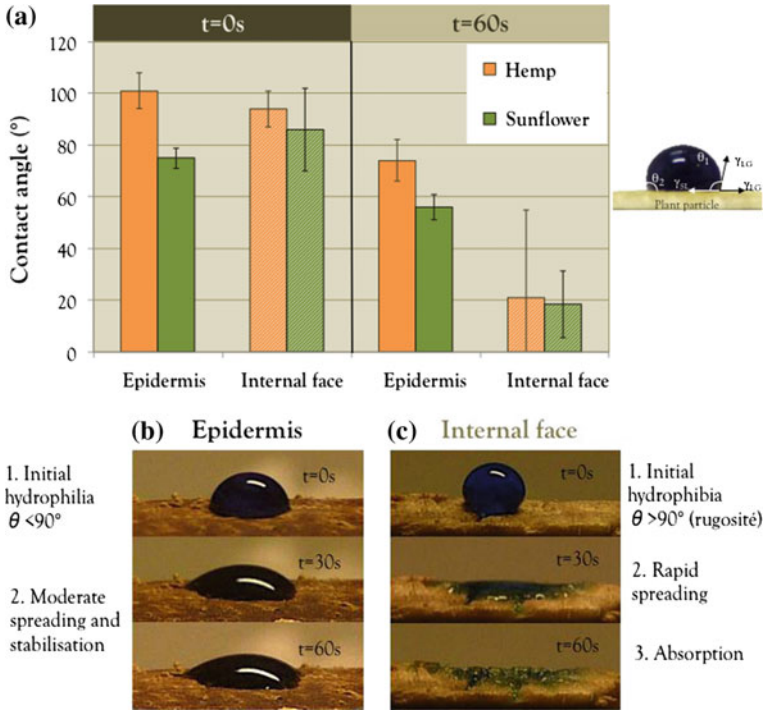

Fig. 3.5 Contact angles formed by a drop of water on the epidermal internal faces of hemp and sunflower particles after 0, 30 and 60 s (**a**). Observation of the characteristic spreading of the drop between 0 and 60 s on the epidermal face (**b**) and the internal face (**c**) of the sunflower

were immersed in mains water (γ_{LG} = 72 mN m^{-1}). The absorption/adsorption curves obtained (Fig. 3.6a) show three successive phases:

- Adsorption of water to the surface of the particle;
- Absorption of water into the internal structure of the particle;
- Gradual diffusion of the trapped air.

The *first phase of surface adsorption* leads to a *near-instantaneous weight gain* W_0 of the chip. This highlights the rapid nature of the wetting of hemp- and sunflower particles, which we saw earlier when we measured the contact angles. Note that the adsorptive weight gain is directly linked to the ratio between the surface area of the granulate and its mass, but also to the surface tension of the liquid in which it is immersed.

The curves themselves (Fig. 3.6a) show, in a *second phase, the absorption in the plant structure*, for which the kinetics *depends on the square root of the elapsed time*. This demonstrates the *diffusive behaviour* of this propagation of water in the structure up to 14 or 24 h. An inflection of the curve relating to the slowing of that diffusion illustrates the influence of the "finite" dimension of the chips. It should be

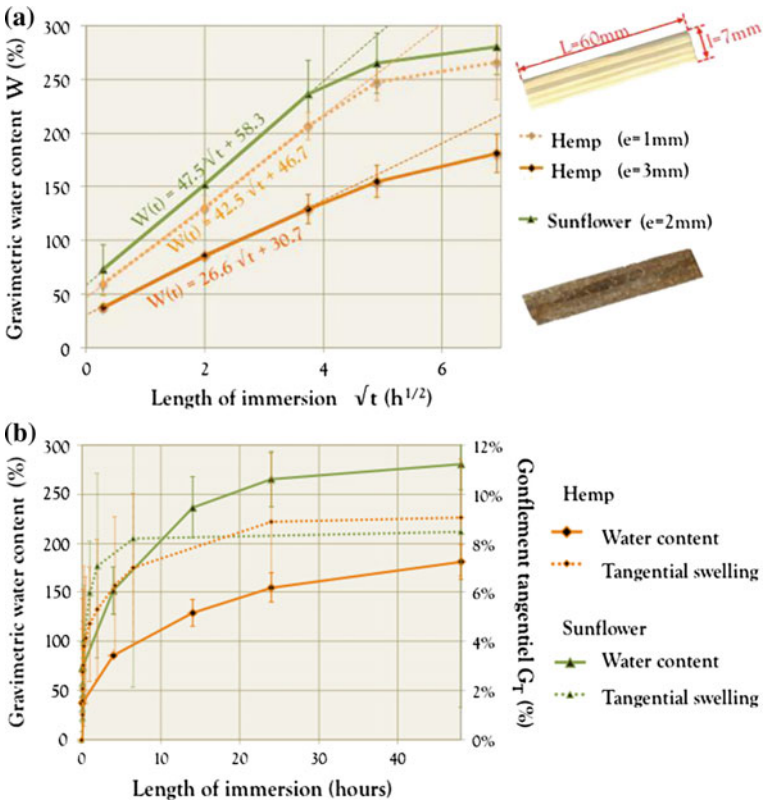

Fig. 3.6 Water adsorption/absorption curve by the immersion of chips (60 × 7 × (1–3) mm^3) of hemp and of sunflower as a function of the square root of elapsed time (**a**). Comparison between the gravimetric water adsorption/absorption and the tangential swelling during immersion (**b**)

noted that the thickness of the chip has a very significant influence on when that slowing starts. A less thick chip tends toward equilibrium more quickly. Hence, diffusion takes place not only in a longitudinal but also in a radial direction.

The *third phase* of the behaviour begins at the start of the inflection on the curve which marks the filling of the particle by the liquid water. This phase corresponds to the *diffusion of the air trapped in the particle* toward the outside, and is extremely slow (AFNOR 1999b).

The phenomenon of adsorption/absorption in the chips before the start of the third phase can therefore be characterised by a simple relation:

$$W(t) = C_A\sqrt{t} + W_0 \tag{3.13}$$

W_0: Initial water adsorption on the surface of the chip [kg kg^{-1}];
C_A: Coefficient of water absorption by the chip [kg $s^{-1/2}$].

Comparing the results between the hemp and sunflower chips highlights the significant capacity for adsorption and absorption of the sunflower granulate. The greater adsorption can be attributed to the rough internal face of the sunflower particles. The available wettable surface is also increased by the multitude of the surfaces provided by the cellulosic marrow, which is shredded during the transformation of the plant material.

The bringing of the plant particles into contact with water, leading to its integration by adsorption/absorption, is responsible for structural swelling. This swelling takes place when water diffuses into the cell walls and forms hydroxide bonds with the hydrophilic compounds such as hemicellulose and cellulose. Figure 3.6b shows that the tangential swelling $G_{T\text{-}SAT}$ is around 9% for pre-dried hemp and sunflower chips. This process is quicker that water absorption, because it takes around 20 h for hemp granulate and 7 h for sunflower granulate to become dimensionally stable. This stabilisation is the sign that the cell walls have reach their fibre saturation point (FSP), which generally lies between 40 and 50% of the initial mass (Rowell 2005).

Adsorption/absorption of divided granulates

The curves of immersion in water for divided granulates of hemp and sunflower (Fig. 3.7a) are of a similar shape to those found in previous works on hemp material (Cerezo 2005; Nguyen et al. 2009a; Arnaud and Gourlay 2012). As is the case with the chips, a first phase of adsorption and a second phase of internal absorption can be seen.

The wetting phase can be considered to have finished after 1 min. The initial adsorption W_0, therefore, will be defined for that duration of immersion. In terms of that value, a significant difference can be seen between the hemp granulate (W_0 = 214.1%) and the sunflower material (W_0 = 362.3%). This too can be attributed, as in the previous section, to the significant roughness of the internal face of the sunflower particles. However, there is an extra factor which comes into play. The divided granulates of hemp and sunflower, have respective specific surfaces estimated at 195 and 226 $cm^2\ g^{-1}$. This larger specific surface of the sunflower granulate also leads to increased initial adsorption. This result is clearly visible when we compare the initial adsorption of that granulate (W_0 = 362.3%) to that of a second sunflower granulate with a smaller specific surface (S_{SPE} = 157 $cm^2\ g^{-1}$). The W_0 then drops by 40%, ending up at the value of 216% because of the specific surface that is 30% lesser.

From Fig. 3.7, it is evident that the absorption of intra-granular water obeys a logarithmic law. This behaviour is due to the particle-size distribution of the granulates, which, as we saw, also obeys a logarithmic distribution. During this absorption phase, the granules become saturated, one by one, starting with the finest and ending with the coarsest. Thus, we can define the following relation, which is valid until the granulates reach saturation:

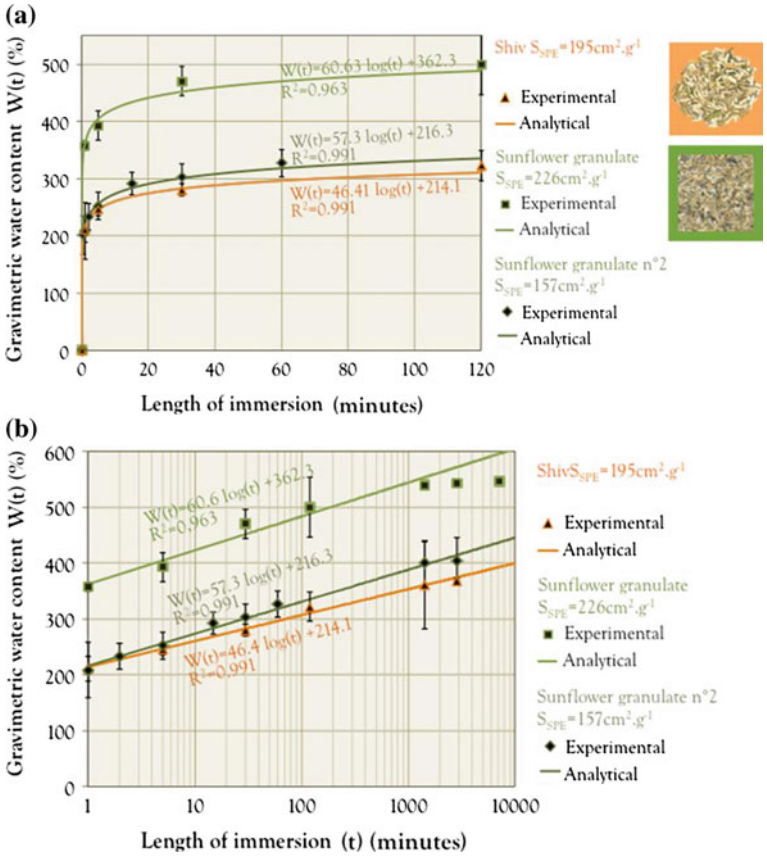

Fig. 3.7 Water adsorption/absorption curves for immersion of hemp and sunflower granulates on a classic timescale (**a**) and on a logarithmic timescale (**b**)

$$W(t) = C_A . \log(t) + W_0 \tag{3.14}$$

W_0: Initial water adsorption on the surface of the granulates;
C_A: Water absorption coefficient of the granulates.

The analytical absorption laws governing the behaviour of granulates report an absorption coefficient that is 30% higher in a sunflower (C_A = 60.6) than a hemp plant (C_A = 46.4). It should be noted that, unlike with surface adsorption, the specific surface has a limited impact on absorption. The sunflower granulate n°2, which has 30% less of a specific surface, thus has absorption kinetics reduced by only 5% (C_A = 57.3).

3.6 Conclusion

In view of the problems relating to water absorption by plant particles, this property has an important factor on the performance of agro-concrete.

It is crucial to understand that the creation of an interface worthy of the name in a composite material, whatever its nature, involves the creation of forces of adhesion between its components.

To date, limited studies have been published on the adhesion between a mineral binder and a lignocellulosic material.

In this chapter, a summary of the adhesion processes and the problems engendered by the combination of a mineral binder and porous lignocellulosic particles is given and the the process of the water as the main problem that needs to be solved.

In this chapter, an overview of the physical laws governing water absorption/adsorption by a plant particle was highlighted. The link with the process of adhesion of a binder to the plant matter was then reported.

The methods used to measure the absorption rate and of the tools used to model it was also described, followed by an analysis of the effect of absorption on the dimensional stability of a particle.

References

AFNOR (b): Méthodes d'essai pour pierres naturelles—Détermination du coefficient d'absorption d'eau par capillarité, AFNOR (1999)

Arnaud, L., Gourlay, E.: Experimental study of parameters influencing mechanical properties of hemp concretes. Constr. Build. Mater. **28**, 50–56 (2012)

Bentz, D.P., Peltz, M.A., Snyder, K.A., Davis, J.M.: VERDiCT: viscosity enhancers reducing diffusion in concrete technology. Concr. Int. **31**, 31–36 (2009)

Bruyne, L.E.: Aspects on wettability and surface composition of modified wood, Doctoral thesis, Manufacturing systems, KTH-Royal Institute of Technology, Stockholm (2008)

Cerezo, V.: Propriétés mécaniques, thermiques et acoustiques d'un matériau à base de particules végétales, Doctoral thesis, INSA de Lyon (2005). http://docinsa.insa-lyon.fr/these/pont.php?id=cerezo, 14 Sept 2010

Coutts, R.S.P., Kightly, P.: Bonding in wood fibre-cement composites. J. Mater. Sci. **19**, 3355–3359 (1984)

Courard, L.: Parametric study for the creation of the interface between concrete and repair products. Mater. Struct. **33**, 65–72 (2000)

De Gennes, P.G., Brochard-Wyard, F., Quéré, D., Reisinger, A.: Capillarity and wetting phenomena: drops, bubbles, pearls, waves, p. 291p. Springer, New York (2004)

Diederich, P., Mouret, M., Ponchon, F.: Design of self-compacting concrete according to the nature of the limestone filler, Actes du congrès SCI 2010, Montreal (Canada) pp. 137–147 (2010)

Einstein, A.: Über die von der molekularkinetischen Theorie der Wärme geforderte Bewegung von in ruhenden Flüssigkeiten suspendierten Teilchen. Ann. Phys. **322**, 549–560 (1905)

Elfordy, S., Lucas, F., Tancret, F., Scudeller, Y., Goudet, L.: Mechanical and thermal properties of lime and hemp concrete ("hempcrete") manufactured by a projection process. Constr. Build. Mater. **22**, 2116–2123 (2008)

Gardner, D.J., Generalla, N.C., Gunnells, D.W., Wolcott, M.P.: Dynamic wettability of wood, Langmuir, vol. 7, pp. 2498–2502, 1 Nov 1991

Groot, C., Larbi, J.: The influence of water flow (reversal) on bond strength development in young masonry. Heron **44**, 63–77 (1999)

Kwasny, J., Sonebi, M., Taylor, S., Bai, Y., Owens, K., Doherty, W.: Influence of the type of coarse lightweight aggregate on properties of semi-lightweight self-consolidating concrete. ASCE Mater. J. Civil Eng. **24**(12), 1474–1483 (2012)

Mounanga, P., Poullain, P., Bastian, G., Glouannec, P., Khelifi, H.: Influence de la composition et du mode de mise en oeuvre sur le développement des propriétés mécaniques du béton de chanvre, Actes du 27ème congrès de l'AUGC, Saint-Malo, 3–5 June 2009. http://www.augc09.univ-rennes1.fr/, 14 Sept 2010

Nguyen, T.T.: Contribution à l'étude de la formulation et du procédé de fabrication d'éléments de construction en béton de chanvre, Doctoral thesis, Université Bretagne Sud (2009a). http://web.univ-ubs.fr/limatb/lab/index.php?option=com_docman&task=doc_download&gid=67, 14 Sept 2010

Nguyen, T.T., Picandet, V., Amziane, S., Baley, C.: Influence of compactness and hemp hurd characteristics on the mechanical properties of lime and hemp concrete. Eur. J. Environ. Civil Eng. **13**, 1039–1050 (2009b)

Nguyen, T.T., Picandet, V., Carre, P., Lecompte, T., Amziane, S., Baley, C.: Effect of compaction on mechanical and thermal properties of hemp concrete. Eur. J. Environ. Civil Eng. **14**, 545–560 (2010)

Rowell, R.: Moisture properties. In: Rowell, R. (ed.) Handbook of Wood Chemistry and Wood Composites, CRC Press, 21p (2005)

Sugo, H.O., Page, A.W., Lawrence, S.J.: The development of mortar/unit bond. In: Proceedings of 9th Canadian Masonry Symposium, Fredericton, 4–6 June 2001

Vick, C.: Adhesive bonding of wood materials. In: Wood Handbook: Wood as an Engineering Material. vol. 113, W. U. F. S. Madison, Ed.: General technical report FPL, pp. 9.1–9.24 (1999)

Walinder, M.: Wetting phenomena on wood—factors influencing measurements of wood wettability, Doctoral thesis, Manufacturing Systems, KTH-Royal Institute of Technology, Stockholm (2000)